Epigenome-wide impact of MAT2A sustains the androgen-indifferent state and confers synthetic vulnerability in ERG fusion-positive prostate cancer

Supplementary Information File

Supplementary Figures 1-9 and legends
Supplementary Table 1

Supplementary Figure 1

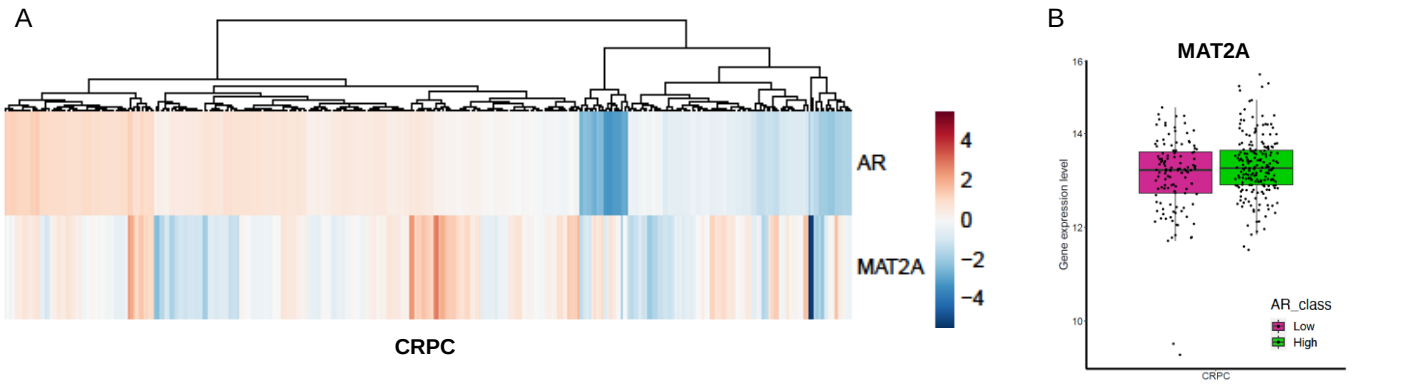

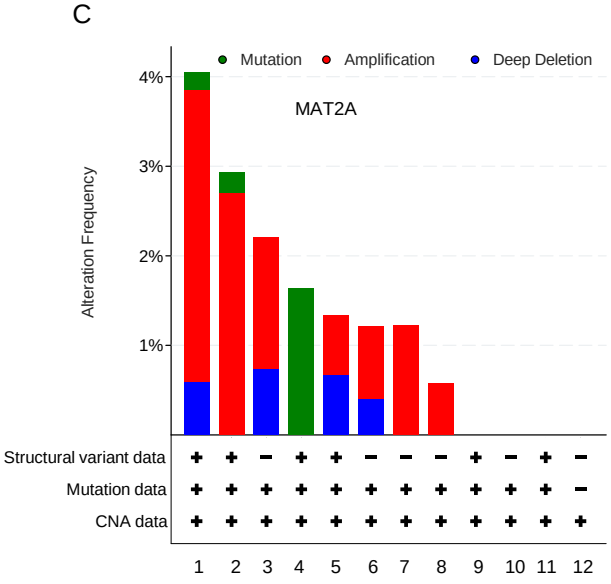

1.Adeno_MSKCC_2018 - Prostate Adenocarcinoma (MSKCC/DFCI, Nature Genetics 2018)
2.Met_SU2C_2019 - Metastatic Prostate adenocarcidoma (SU2C/PCF Dream team, PNAS 2019)
3.Adeno_Hutch - Prostate Adenocarcinoma (Fred Hutchinson CRC, Nat Med 2016)
4.Met_MCTP - Metastatic Prostate Adenocarcinoma (MCTP, Nature 2012)
5.Met_SU2C_2015 - Metastatic Prostate Cancer (SU2C/PCF Dream team, Cell 2015)
6.Adeno_TCGA - Prostate Adenocarcinoma (TCGA, Firehouse Legacy)
7.Met_Prov - The Metastatic Prostate Cancer Project (Provisional, June 2021)
8.Adeno_ MSKCC_2010 - Prostate Adenocarcinoma (MSKCC, Cancer Cell 2010)
9.Adeno_Broad_2013 - Prostate Adenocarcinoma (Broad/Cornell, Cell 2013)
10.Adeno_Broad_2012 - Prostate Adenocarcinoma (Broad/Cornell, Nat Genet 2012)
11.Adeno_SMMU - Prostate Adenocarcinoma (SMMU, Eur Urol 2017)
12.Adeno_MSKCC_2017 - Prostate Cancer (MSKCC, JCO Precis Oncol 2017)

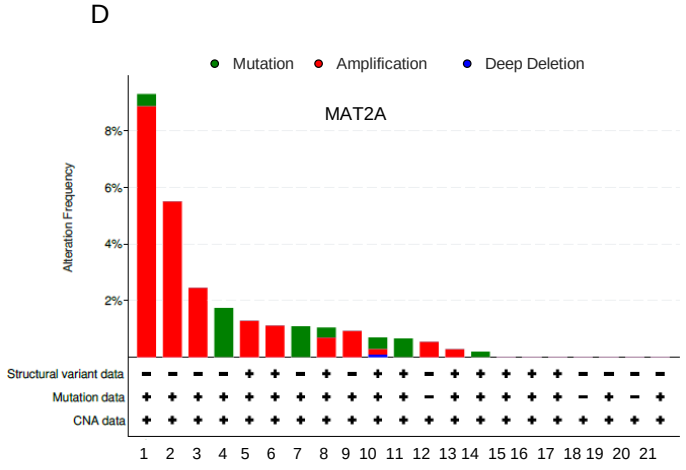

1.The Metastatic Breast Cancer Project (Provisional, February 2020)
2.Pancreatic Cancer (UTSW, Nat Commun 2015)
3.Proteogenomic landscape of breast cancer (CPTAC, Cell 2020)
4.Liver Hepatocellular Carcinoma (AMC, Hepatology 2014)
5.Lung Squamous Cell Carcinoma (TCGA, PanCancer Atlas)
6.Adrenocortical Carcinoma (TCGA, PanCancer Atlas)
7.Lung Adenocarcinoma (Broad, Cell 2012)
8.Pan-Lung Cancer (TCGA, Nat Genet 2016)
9.Metastatic Breast Cancer (INSERM, PLoS Med 2016)
10.Breast Invasive Carcinoma (TCGA, PanCancer Atlas)
11.Lung Adenocarcinoma (OncoSG, Nat Genet 2020)
12.Breast Cancer (METABRIC, Nature 2012 & Nat Commun 2016)
13.Liver Hepatocellular Cercinoma (TCGA, PanCancer Atlas)
14.Lung Adenocarcinoma (TCGA, PanCancer Atlas)
15.Adenoid Cystic Carcinoma Project (J Clinic Invest 2019)
16.Pancreatic Adenocarcinoma (TCGA, PanCancer Atlas)
17.Adenoid Cystic Carcinoma of the Breast (MSKCC, J Pathol. 2015)
18.Breast Cancer (MSK, Nature Cancer 2020)
19.Breast Cancer (MSKCC, NP J Breast Cancer 2019)
20.Liver Hepatocellular Adenoma and Carcinomas (MSK, PLoS One 2018)
21.Lung Adenocarcinoma (CPTAP, Cell 2020)

Supplementary Figure 1. MAT2A is frequently altered in several type of tumors and in prostate cancer.

A) Heatmap of AR and MAT2A expression values in the cohort of CRPC patients described in Figure 1A. B) Gene expression level of MAT2A in CRPC described above and divided in AR high (n=118) and AR low (n=198) expressing patients. For box-and-whisker plots, the line inside the box shows the median value. The bounds of the box represent the 25th–75th percentiles, with whiskers at minimum and maximum values. C) Cbioportal database search of MAT2A amplification, deletion and mutations in several types of prostate cancer; cases with mutations and copy number alterations were reported. D) Cbioportal database search of MAT2A amplification, deletion and mutations in several cancer types. Dataset includes 8420 patients, 8483 samples in 21 studies; cases with mutations and copy number alterations were reported.

Supplementary Figure 2

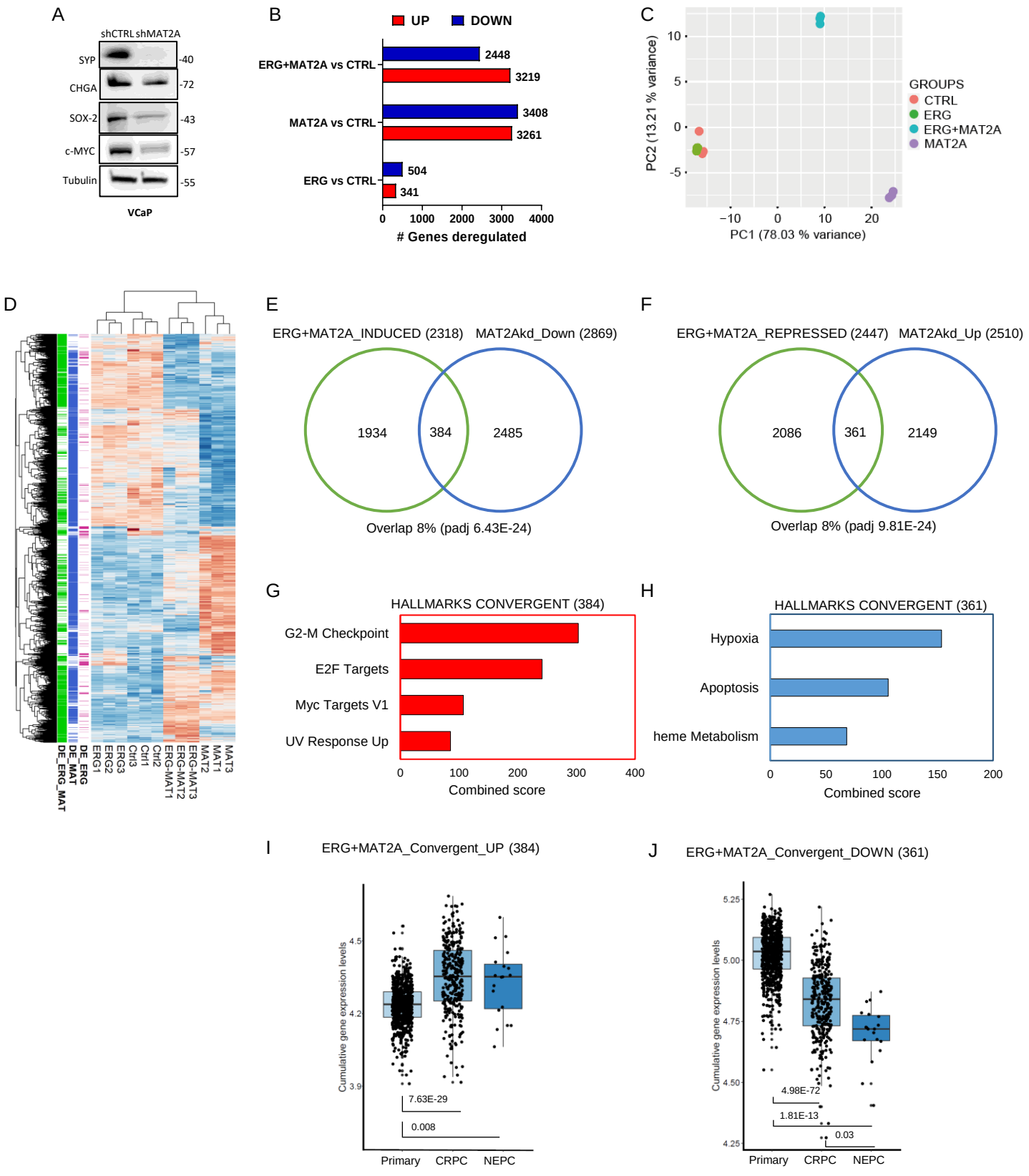

Supplementary Figure 2. Transcriptional impact of ERG and MAT2A alone and in combination in RWPE-1 cells.

A) Immunoblot with indicated Ab in MAT2Akd VCaP cells (n=2 independent experiments). B) Number of genes affected by ERG and MAT2A expression in RWPE-1 cells, alone or in combination (p-value ≤ 0.05). C) PCA plot of RWPE-1 cell lines, colored according to the condition (CTRL, ERG, MAT2A, and ERG+MAT2A together). D) Heatmap of differentially expressed genes in the indicated RWPE-1 cell lines. Replicates are indicated. E) Convergence analyses between genes upregulated in RWPE-1 ERG+MAT2A and genes downregulated in VCaP MAT2Akd cells (Sh1 and Sh2). F) Convergence analyses between genes downregulated in RWPE-1 ERG+MAT2A and genes upregulated in VCaP MAT2Akd cells (Sh1 and Sh2). G) Significantly enriched pathways in genes upregulated in RWPE-1 ERG+MAT2A and genes downregulated in VCaP MAT2Akd cells (Sh1 and Sh2) performed with enrichR. H) Significantly enriched pathways in genes downregulated in RWPE-1 ERG+MAT2A and genes upregulated in VCaP MAT2Akd cells (Sh1 and Sh2) performed with enrichR. I) Cumulative expression level of genes up-regulated in ERG+MAT2A and convergent with repressed by MAT2Akd in VCaP cells (384 genes) in the cohort of primary, CRPC and NEPC patients. J) Cumulative expression level of genes down-regulated in ERG+MAT2A and convergent with induced by MAT2Akd in VCaP cells (361) in the cohort of primary, CRPC and NEPC patients. Primary, n=714; CRPC, n=316; NEPC, n=19. For box-and-whisker plots in (I) and (J), the line inside the box shows the median value. The bounds of the box represent the 25th–75th percentiles, with whiskers at minimum and maximum values. One-way-ANOVA was used to test significant differences between groups.

Supplementary Figure 3

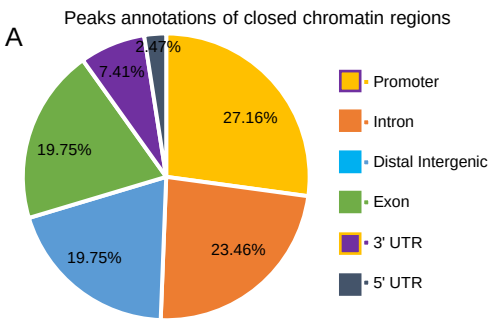

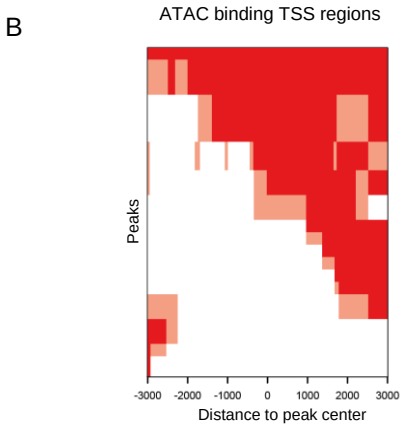

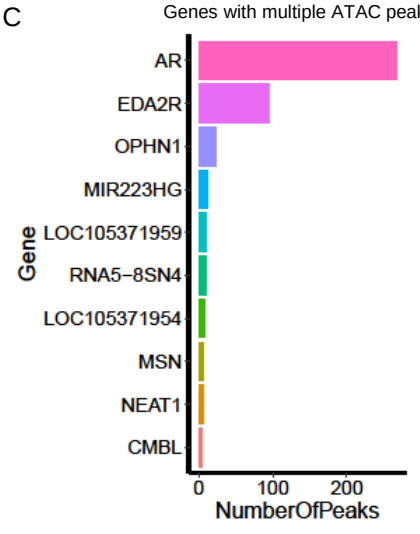

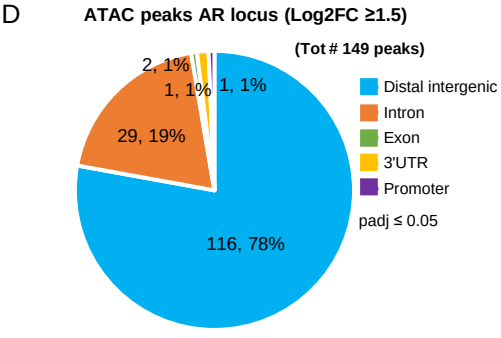

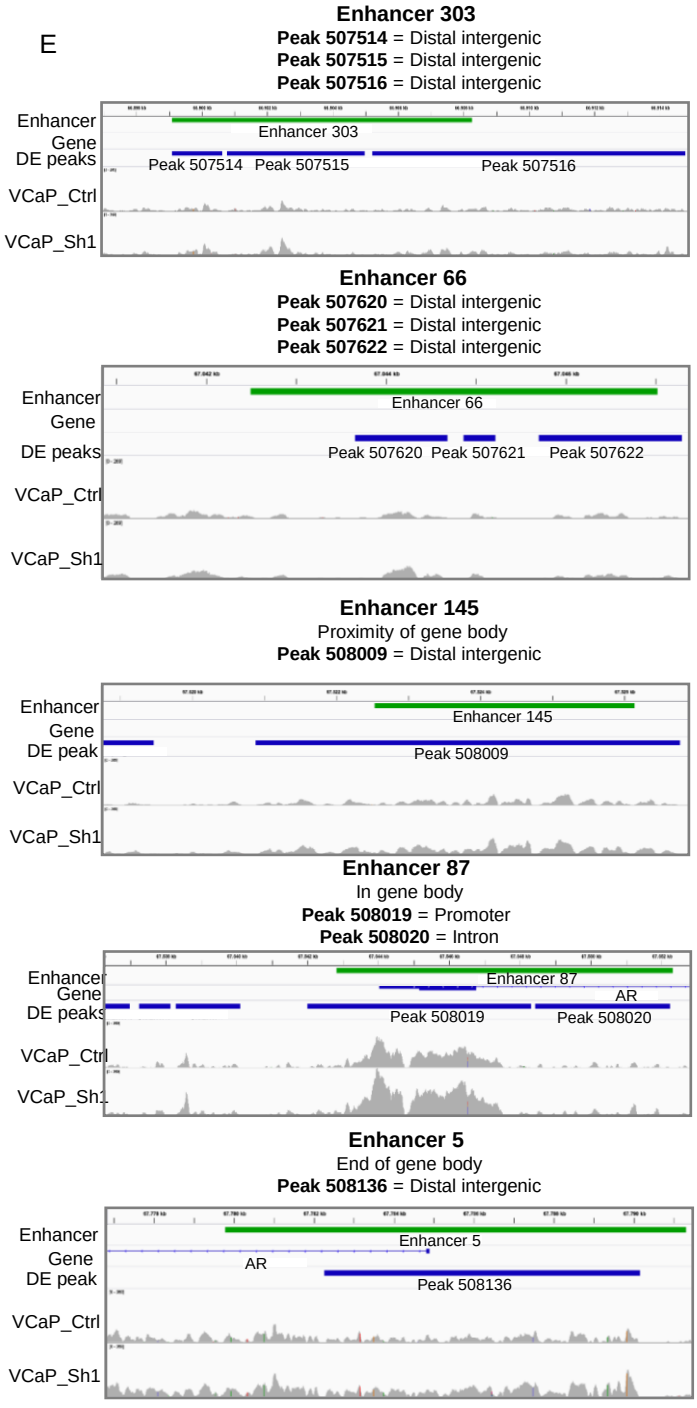

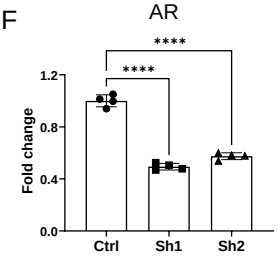

Supplementary Figure 3. MAT2A controls chromatin conformation.
A) Distribution of the annotated peaks in the closed regions. B) Peak location in TSS regions. C) Genes with multiple ATAC-seq peaks. D) Percentage and location of open peaks identified by ATAC-seq at the AR locus (Log2FC ≥1.5). E) Focused view on the enhancer regions with location of significantly open peaks. The 5 enhancer are indicated. F) mRNA level of AR gene in VCaP MAT2Akd versus Ctrl cells (n=4 biological replicates). All error bars, mean ± s.d. ****p < 0.0001. One-way-ANOVA was used to test significant differences between groups.

Supplementary Figure 4

A

	Log2FC	P-value
H3K4me1	-0.12	0.77
H3K4me2	-3.03	0.02
H3K9me1	-0.45	0.23
H3K9me2	0.60	0.04
H3K9me3	0.60	0.05
H3K14me1	-0.37	0.48
H3K14me2	2.45	0.01
H3K18me1	-0.74	0.15
H3K23me1	-0.73	0.27
H3K27me1	-0.63	0.10
H3K27me2	-0.87	0.10
H3K27me3	-0.69	0.14
H3K36me1	-0.64	0.14
H3K36me2	-0.87	0.05
H3K36me3	-1.34	0.02
H3K79me1	1.03	0.28
H3K79me2	-0.11	0.91

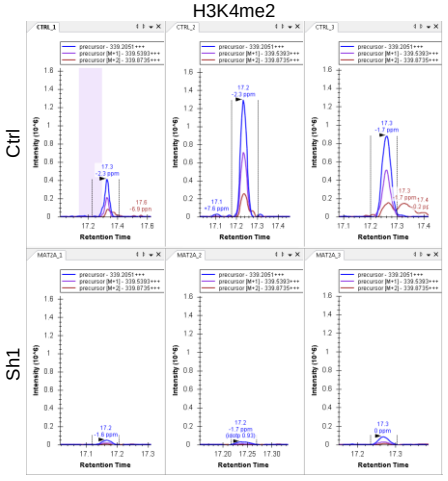

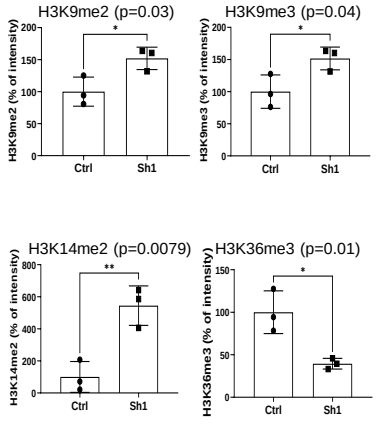

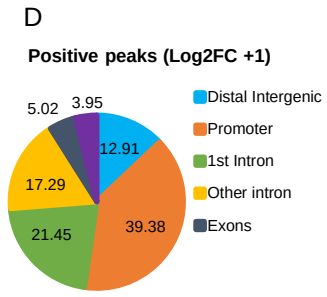

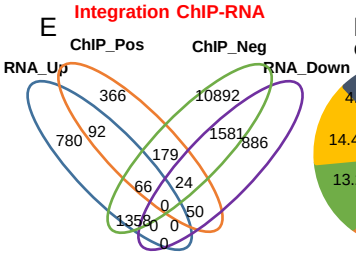

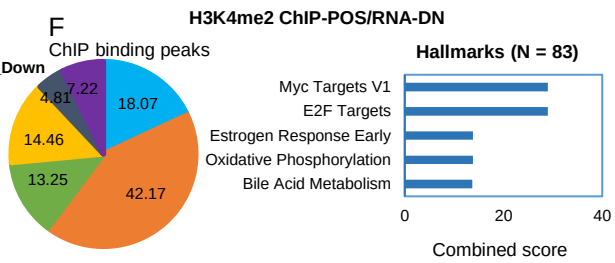

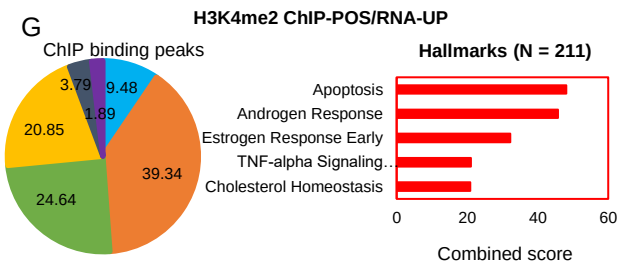

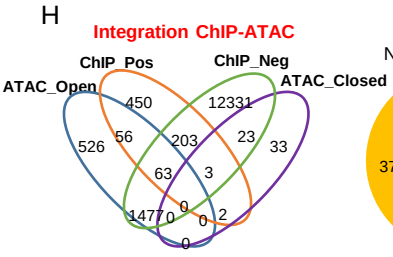

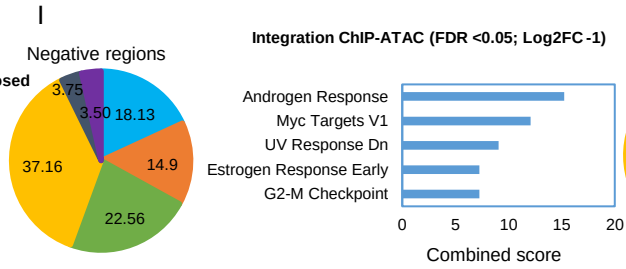

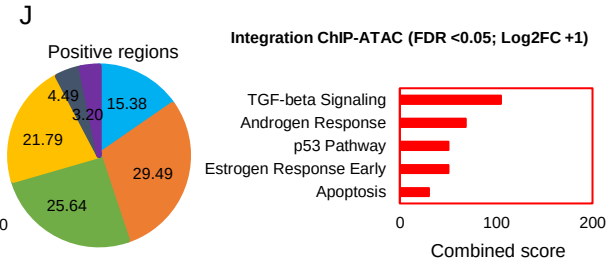

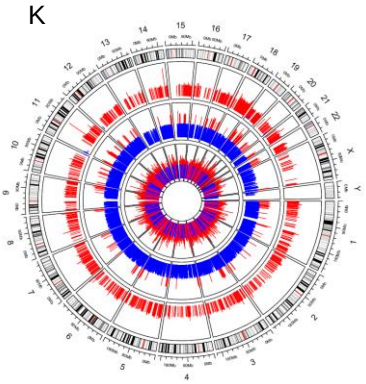

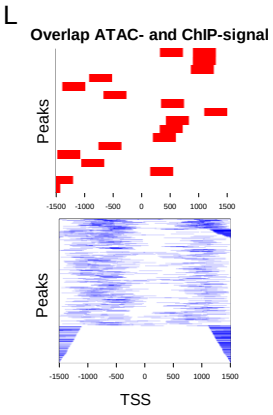

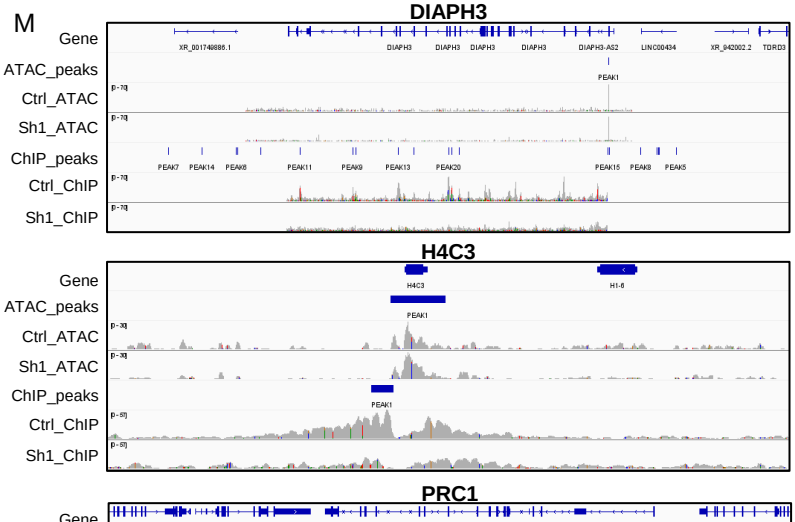

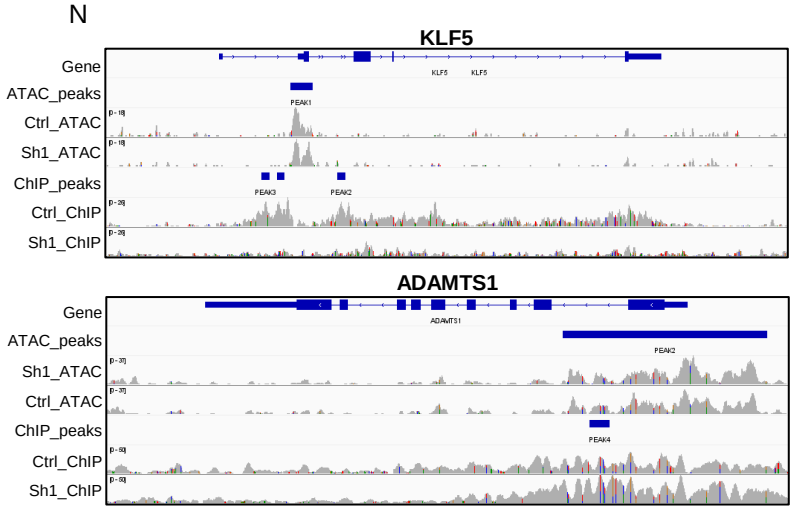

Supplementary Figure 4. MAT2A controls chromatin accessibility and enhances histone 3 lysine 4 di-methylation

A) List of all the H3 markers evaluated by high-resolution mass spectrometry analysis in VCaP cells control (Ctrl) and MAT2Akd (Sh1). Log2FC (Sh1 vs Ctrl) and p-values are reported. B) Left, high-resolution mass spectrometry (MS) profiles of H3K4me2 in the replicates of VCaP control (Ctrl) and MAT2Akd (Sh1). C) Percentage of intensity score of the indicated markers in VCaP MAT2Akd (Sh1) compared to control (Ctrl) (n=3 biological replicates). D) Distribution of positive H3K4me2 peaks in VCaP MAT2Akd cells. E) Venn diagram showing integration between ChIP-seq and RNA-seq data in VCaP MAT2Akd cells compared to VCaP Ctrl cells. F) Peak annotation (Left) and Hallmarks (Right), of the genes with positive ChIP-seq peak and reduced expression in RNA-seq. G) Peak annotation (Top) and Hallmarks (Bottom), of genes with positive ChIP-seq peaks and enhanced expression in RNA-seq. H) Venn diagram showing integration between ChIP-seq and ATAC-seq data in VCaP MAT2Akd cells compared to VCaP Ctrl cells. I) Peak annotation (Left) and Hallmarks (Right), of the genes with negative ChIP-seq peak and closed ATAC-seq peaks. J) Peak annotation (Left) and Hallmarks (Right) of the genes with positive ChIP-seq peak and open ATAC-seq peaks. K) Circular plot of the integrative analysis ChIP-seq/ATAC-seq/RNA-seq showing the distribution of the differentially expressed peaks (outer layer), the differentially distributed H3K4me2 peaks (middle) and the significantly expressed genes (inner layer). L) Heatmap showing overlap between ATAC-seq and ChIP-seq peaks. M) ChIP-seq and ATAC-seq peaks at down-regulated genes in VCaP MAT2Akd and VCaP control samples. Plot were generated through IGV software as described in Figure 3G. N) ChIP-seq and ATAC-seq peaks at up-regulated genes in VCaP MAT2Akd and VCaP control samples. Plot were generated through IGV software as described in Figure 3G. All error bars, mean ± s.d. *$p < 0.05$, **$p < 0.01$. One-way-ANOVA was used to test significant differences between groups.

Supplementary Figure 5

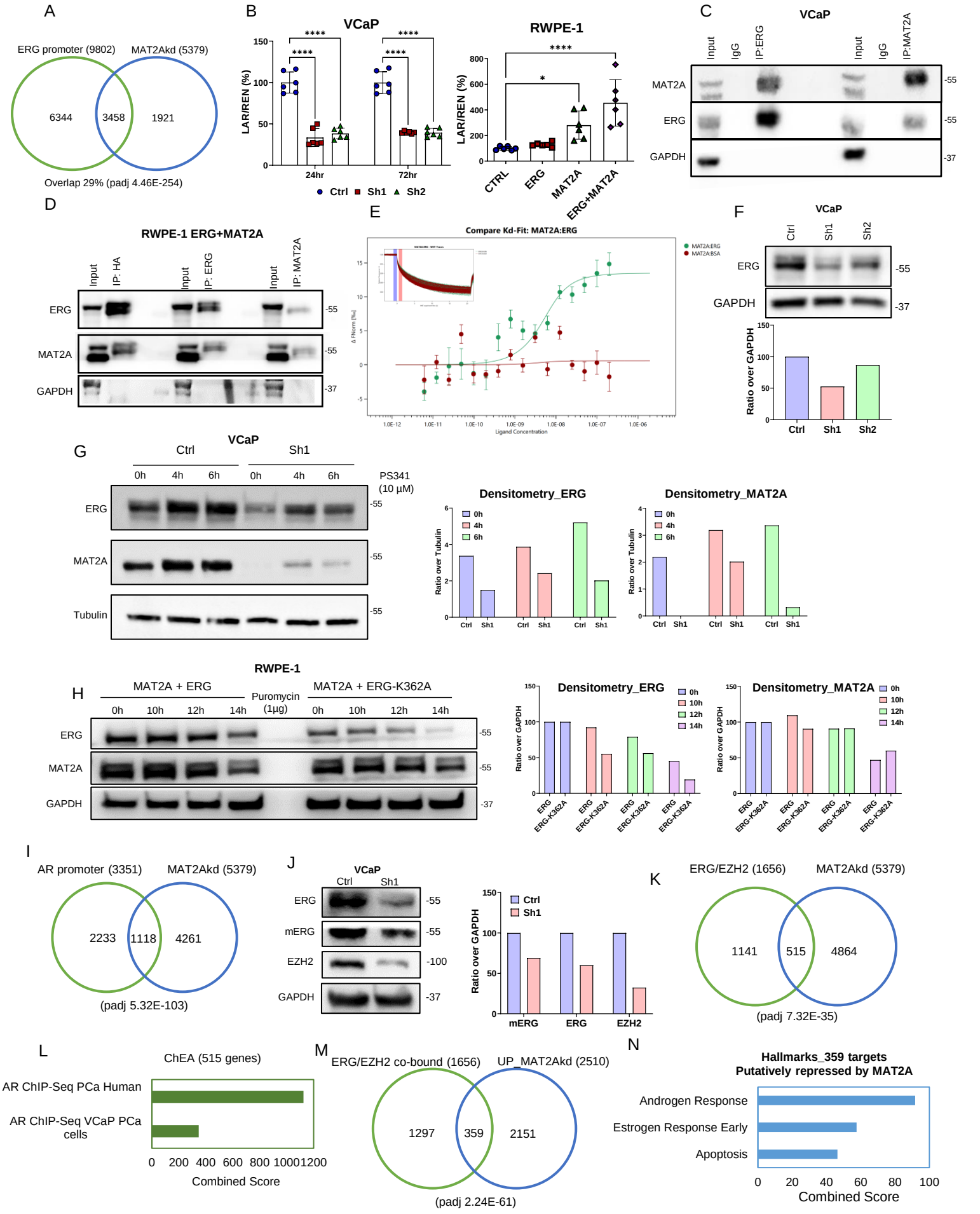

Supplementary Figure 5. MAT2A interacts with ERG altering ERG/EZH2/AR crosstalk.
A) Venn diagram showing the overlap between deregulated genes in VCaP MAT2Akd cells and genes bound by ERG in their promoter. B) Luciferase assay showing ETS promoter activity in VCaP MAT2Akd cells (left) and RWPE-1 overexpressing ERG, MAT2A or both (right) (n=6 biological replicates). C) Evaluation of ERG-MAT2A interaction by immunoprecipitation in VCaP cells using indicated Ab (n=2 independent experiments). D) Evaluation of ERG-MAT2A interaction by immunoprecipitation in RWPE-1 ERG+MAT2A cells using indicated Ab (n=2 independent experiments). E) Evaluation of ERG-MAT2A interaction by MST. Difference between MST signal of target and complex in ‰ Fnorm units. Green curve represents binging of MAT2A and ERG, while red curve represents negative control showing no binding affinity between MAT2A and BSA. MST signal of target and complex in normalized Δ‰ Fnorm units. Binding affinity (Kd) between MAT2A and ERG was calculated at 2,66 nM (± 2,35 nM). Insert, MST tracing (n=2 biological replicates). F) Evaluation of ERG protein level in VCaP Ctrl and MAT2Akd VCaP cells (Sh1, Sh2) by immunoblots in indicated cell lines. Bottom, densitometry analysis of the indicated markers (n=3 independent experiments). G) MAT2Akd reduces ERG stability by enhancing ERG proteosomal degradation. ERG stabilization by the proteosomal inhibitor (PS341, 10μM) at different time points (0h, 4h or 6h) in VCaP control (Ctrl) and MAT2Akd (Sh1). Left, densitometry analysis of the indicated markers (n=2 independent experiments). H) Immunoblot of indicated Ab in RWPE-1 transfected with MAT2A and ERG or ERG-K362A plasmids, treated with 1μg of puromycin at different time points. Right densitometry analysis of the indicated markers (n=2 independent experiments). I) Venn diagram showing the overlap between deregulated genes in VCaP MAT2Akd cells and genes bound by AR in their promoter. J) Immunoblot of EZH2, ERG and methylated ERG in VCaP Control (Ctrl) and MAT2Akd (Sh1) cells. Right, densitometry analysis of the indicated markers (n=3 independent experiments). K) Venn diagram showing the convergence between genes co-occupied by ERG/EZH2 and those deregulated by MAT2Akd. L) ChEA enrichment of the 515 shared genes convergent as described in S5J. M) Convergence of ERG-EZH2 co-occupied targets and genes upregulated by MAT2Akd (i.e. repressed by MAT2A). N) Hallmarks of shared 359 targets (putatively repressed by MAT2A). Molecular weights are indicated in kilodaltons (kDa). All error bars, mean ± s.d. *$p < 0.05$, ****$p < 0.0001$. One-way-ANOVA was used to test significant differences between groups.

Supplementary Figure 6

A

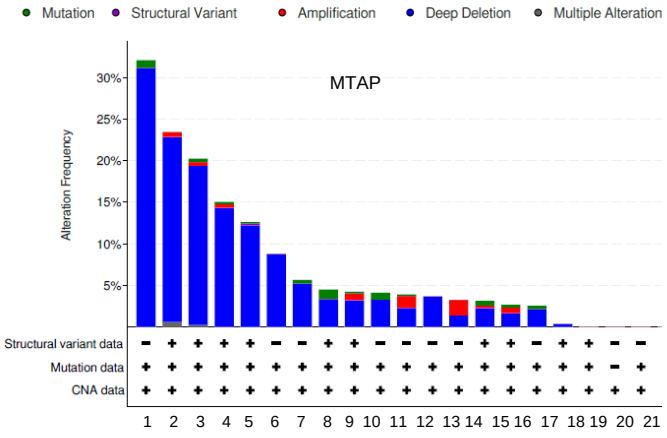

1.Pancreatic Cancer (UTSW, Nat Commun 2015)
2.Pancreatic Adenocarcinoma (TCGA, PanCancer Atlas)
3.Lung Squamous Cell Carcinoma (TCGA, PanCancer Atlas)
4.Pan-Lung Cancer (TCGA, Nat Genet 2016)
5.Lung Adenocarcinoma (TCGA, PanCancer Atlas)
6.Lung Adenocarcinoma (Broad, Cell 2012)
7.Liver Hepatocellular Carcinoma (AMC, Hepatology 2014)
8.Adrenocortical Carcinoma (TCGA, PanCancer Atlas)
9.Breast Invasive Carcinoma (TCGA, PanCancer Atlas)
10.Proteogenomic landscape of breast cancer (CPTAC, Cell 2020)
11.Breast Cancer (METABRIC, Nature 2012 & Nat Commun 2016)
12.Lung Adenocarcinoma (CPTAP, Cell 2020)
13.Metastatic Breast Cancer (INSERM, PLoS Med 2016)
14.Liver Hepatocellular Cercinoma (TCGA, PanCancer Atlas)
15.Lung Adenocarcinoma (OncoSG, Nat Genet 2020)
16.The Metastatic Breast Cancer Project (Provisional, February 2020)
17.Adenoid Cystic Carcinoma Project (J Clinic Invest 2019)
18.Adenoid Cystic Carcinoma of the Breast (MSKCC, J Pathol. 2015)
19.Breast Cancer (MSK, Nature Cancer 2020)
20. Breast Cancer (MSKCC, NP J Breast Cancer 2019)
21. Liver Hepatocellular Adenoma and Carcinomas (MSK, PLoS One 2018)

B

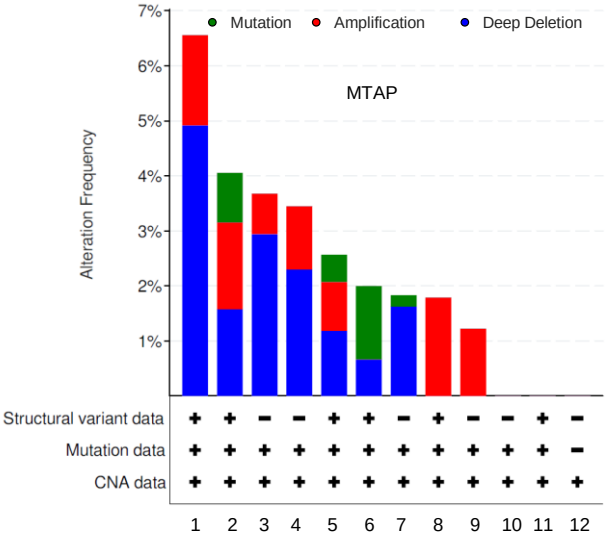

1.Met_MCTP - Metastatic Prostate Adenocarcinoma (MCTP, Nature 2012)
2.Met_SU2C_2019 - Metastatic Prostate adenocarcidoma (SU2C/PCF Dream team, PNAS 2019)
3.Adeno_Hutch - Prostate Adenocarcinoma (Fred Hutchinson CRC, Nat Med 2016)
4.Adeno_ MSKCC_2010 - Prostate Adenocarcinoma (MSKCC, Cancer Cell 2010)
5.Adeno_MSKCC_2018 - Prostate Adenocarcinoma (MSKCC/DFCI, Nature Genetics 2018)
6.Met_SU2C_2015 - Metastatic Prostate Cancer (SU2C/PCF Dream team, Cell 2015)
7.Adeno_TCGA - Prostate Adenocarcinoma (TCGA, Firehouse Legacy)
8.Adeno_Broad_2013 - Prostate Adenocarcinoma (Broad/Cornell, Cell 2013)
9.Met_Prov - The Metastatic Prostate Cancer Project (Provisional, June 2021)
10.Adeno_Broad_2012 - Prostate Adenocarcinoma (Broad/Cornell, Nat Genet 2012)
11.Adeno_SMMU - Prostate Adenocarcinoma (SMMU, Eur Urol 2017)
12.Adeno_MSKCC_2017 - Prostate Cancer (MSKCC, JCO Precis Oncol 2017)

C

Prostate cancer cell lines	MTAP alterations
NCI-H660	No
VCaP	No
MDAPCA2B	No
DU145	No
LNCaP (clone FGC)	No
PC3	No
PRECLH	No

D

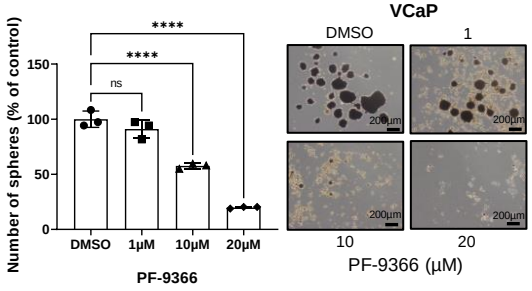

E

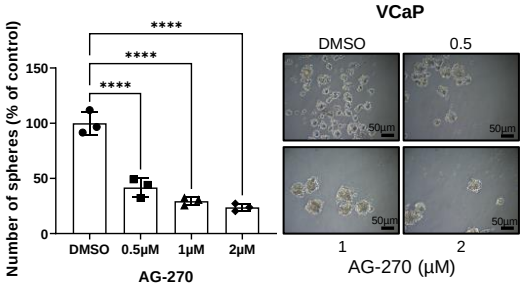

F

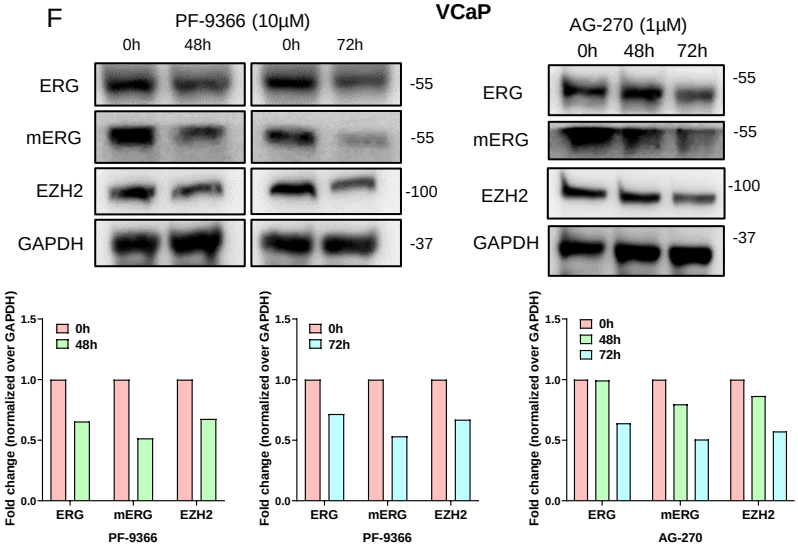

G

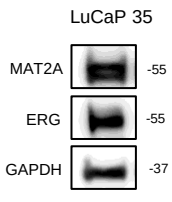

H

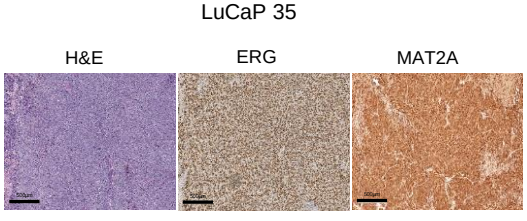

I

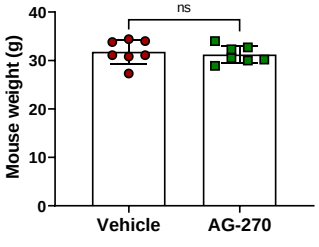

Supplementary Figure 6. MAT2A inhibitors reverse the malignant phenotype in vitro and in vivo independently from MTAP deletion.

A) Cbioportal database search of MTAP amplification, deletion and mutations in several cancer types including Liver, Lung, Pancreas, Breast, Bone, Adrenal Gland. This dataset includes 8420 patients, 8483 samples in 21 studies; only the cases for which both the mutations and copy number alterations data are available were reported. B) Cbioportal database search of MTAP amplification, deletion and mutations in several types of prostate cancer (only the cases for which both the mutations and copy number alterations data are available are reported). C) Cbioportal database search of MTAP alterations in indicated prostate cancer cell lines. D) SFA assay in VCaP cells treated with the indicated doses of PF-9366 (n=3 biological replicates). Right, representative images are shown. Scale bars are 200µm. E) SFA assay in VCaP cells treated with the indicated doses of AG-270 (n=3 biological replicates). Right, representative images are shown. Scale bars are 50µm. F) Immunoblot of EZH2, ERG and methylated ERG in VCaP cells following time course treatment (48h and 72h) with the indicated concentration of PF-9366 (left) and AG-270 (right). Bottom, densitometry analysis of indicated markers (n=2 independent experiments). For mERG evaluation a duplicate loading in the same gel was performed to process samples in parallel. G) Immunoblot of lysates from LuCaP 35 tumors with indicated markers. Molecular weights are indicated in kilodaltons (kDa) (n=2 independent experiments). H) H&E and immunohistochemical evaluation of MAT2A and ERG in LuCaP 35. Scale bars are 500µm. I) Mouse weight of indicated mice (n=7/group) groups carrying LuCaP 35. All error bars, mean ± s.d. n.s.= not significant, ****$p < 0.0001$. One-way-ANOVA was used to test significant differences between groups.

Supplementary Figure 7

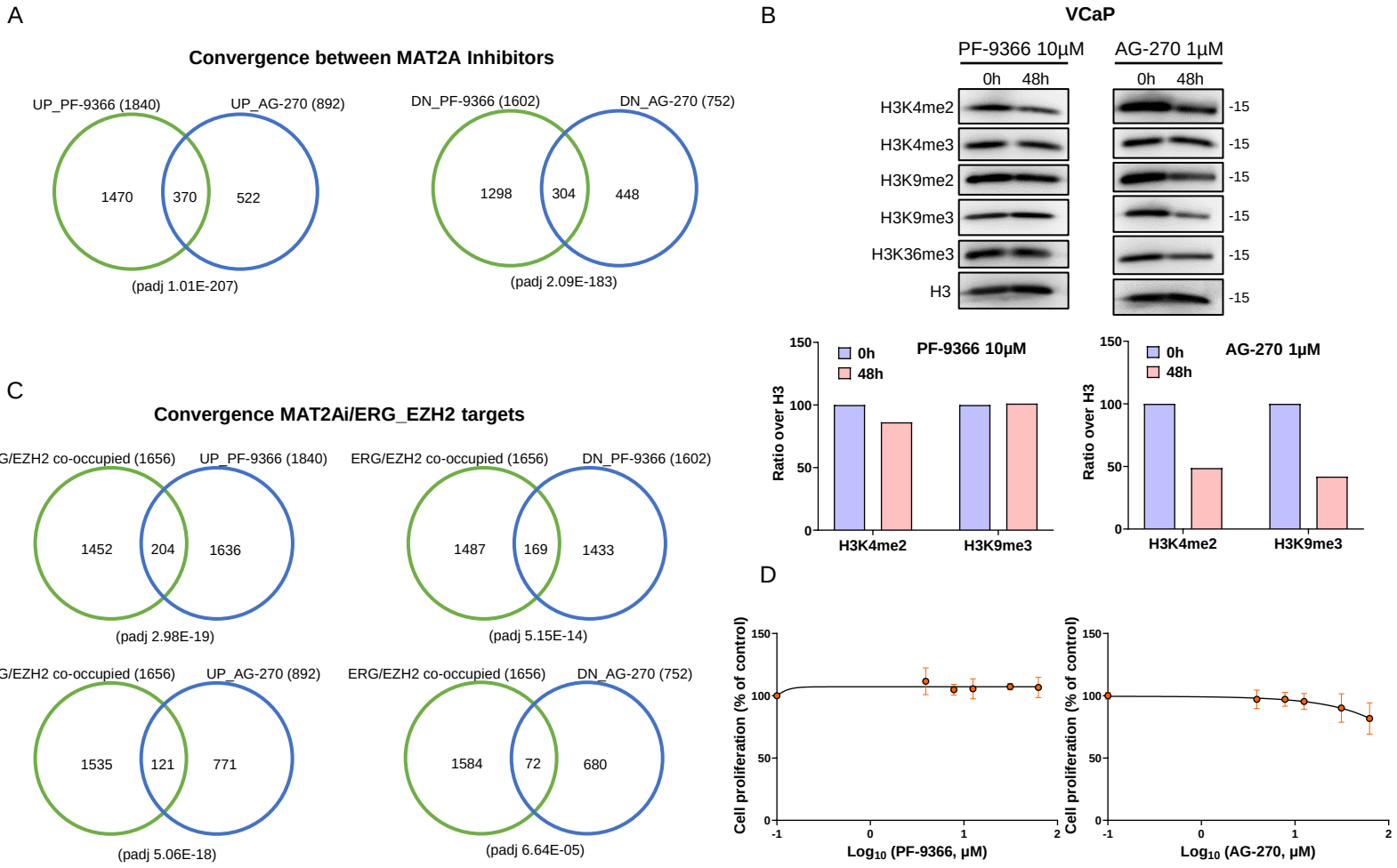

Supplementary Figure 7. Transcriptional and epigenetic impact of MAT2A inhibitors.
A) Venn diagram showing overlap between genes deregulated by PF-9366 and AG-270. Left, overlap between upregulated genes. Right, overlap between down-regulated genes. B) Immunoblot of selected histone PTM marks in VCaP cells following treatment with the indicated concentration of PF-9366 (left) and AG-270 (right) (n=3 independent experiments). C) Convergence between MAT2Ai and ERG/EZH2 deregulated targets (threshold on Log2FC ±0.1). Up-regulated and down-regulated genes as indicated. Top, overlap with genes deregulated by PF-9366. Bottom, overlap with genes deregulated by AG-270. D) SRB proliferation assay in RWPE-1 cells treated with increasing doses of PF-9366 (left) and AG-270 (right) (n=3 biological replicates). Molecular weights are indicated in kilodaltons (kDa). All error bars, mean ± s.d.

Supplementary Figure 8

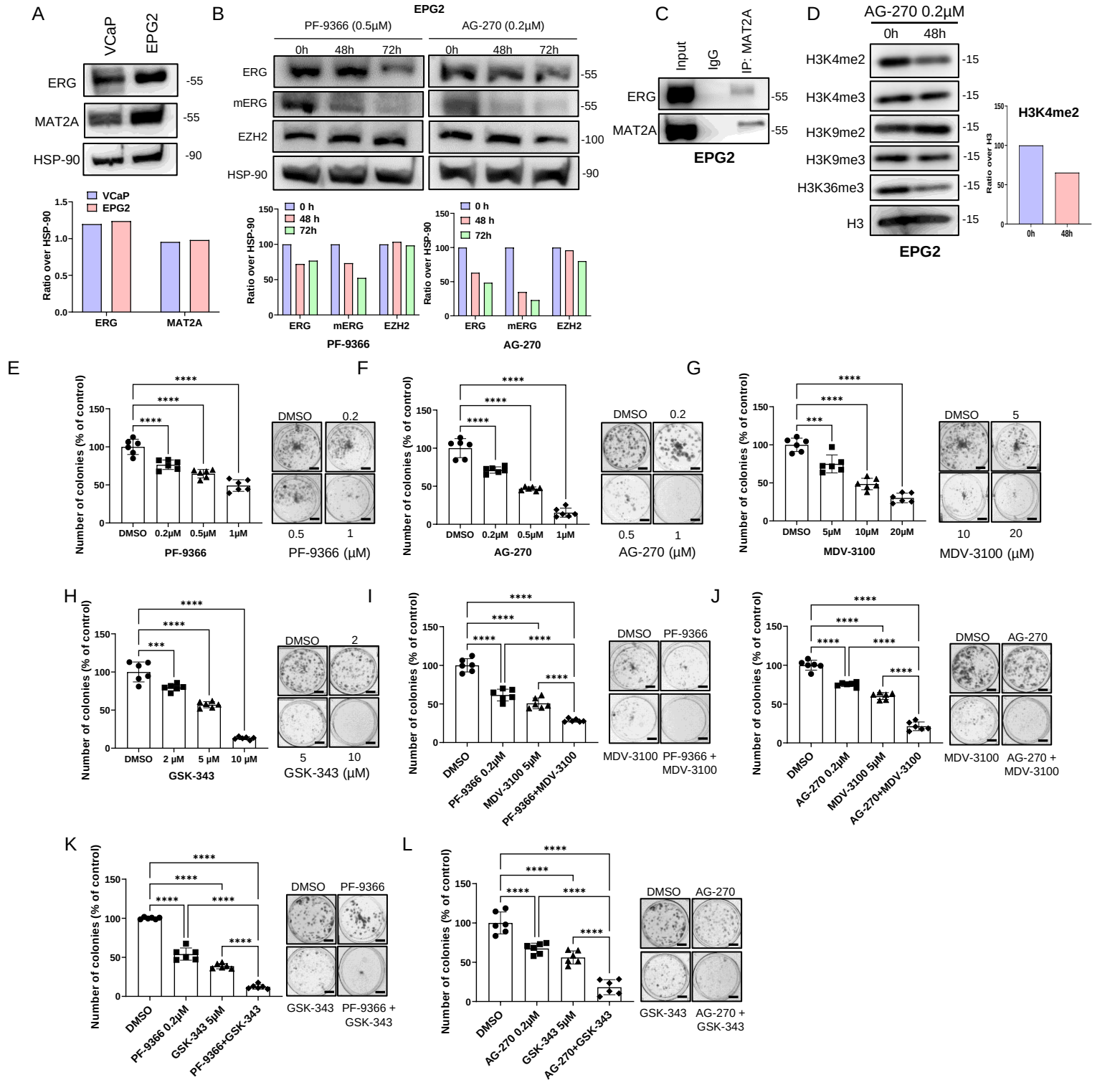

Supplementary Figure 8. MAT2A inhibition reverse aggressive features in EPG2 cells alone and in combination with GSK-343 and MDV-3100.

A) Immunoblot analysis showing ERG and MAT2A expression in EPG2 cells, compared to VCaP cells. Bottom, densitometry analysis of indicated Ab. (n=2 independent experiments) B) Immunoblot of ERG, methylated ERG and EZH2 in EPG2 cells following time course treatment (48h and 72h) with the indicated concentration of PF-9366 (left) and AG-270 (right). For mERG evaluation a duplicate loading in the same gel was performed to process samples in parallel. Bottom, densitometry analysis of indicated Ab. (n=2 independent experiments) C) Evaluation of ERG-MAT2A interaction by immunoprecipitation in EPG2 cells using indicated Ab. Right, densitometry analysis of H3K4me2. (n=2 independent experiments D) Immunoblot of the indicated Ab in EPG2 cells treated with AG-270. (n=2 independent experiments E) Colony formation assay in EPG2 cells treated with the indicated concentration of PF-9366 (n=6 biological replicates). Right, representative images are shown. F) Colony formation assay in EPG2 cells treated with the indicated concentration of AG-270 (n=6 biological replicates). Right, representative images are shown. G) Colony formation assay in EPG2 cells treated with the indicated concentration of MDV-3100 (n=6 biological replicates). Right, representative images are shown. H) Colony formation assay in EPG2 cells treated with the indicated concentration of GSK-343 (n=6 biological replicates). Right, representative images are shown. I) Colony formation assay in EPG2 cells treated with the indicated concentration of PF-9366 and MDV-3100, alone or in combination (n=6 biological replicates). Right, representative images are shown. J) Colony formation assay in EPG2 cells treated with the indicated concentration of AG-270 and MDV-3100, alone or in combination (n=6 biological replicates). Right, representative images are shown. K) Colony formation assay in EPG2 cells treated with the indicated concentration of PF-9366 and GSK-343, alone or in combination (n=6 biological replicates). Right, representative images are shown. L) Colony formation assay in EPG2 cells treated with the indicated concentration of AG-270 and GSK-343, alone or in combination (n=6 biological replicates). Right, representative images are shown. Molecular weights are indicated in kilodaltons (kDa). For all the colony-forming assays (E-L) images of 12-well plates are shown. Scale bars, 5 mm. All error bars, mean ± s.d. ***$p < 0.001$ ****$p < 0.0001$. One-way ANOVA was used to test significant differences between groups.

Supplementary Figure 9

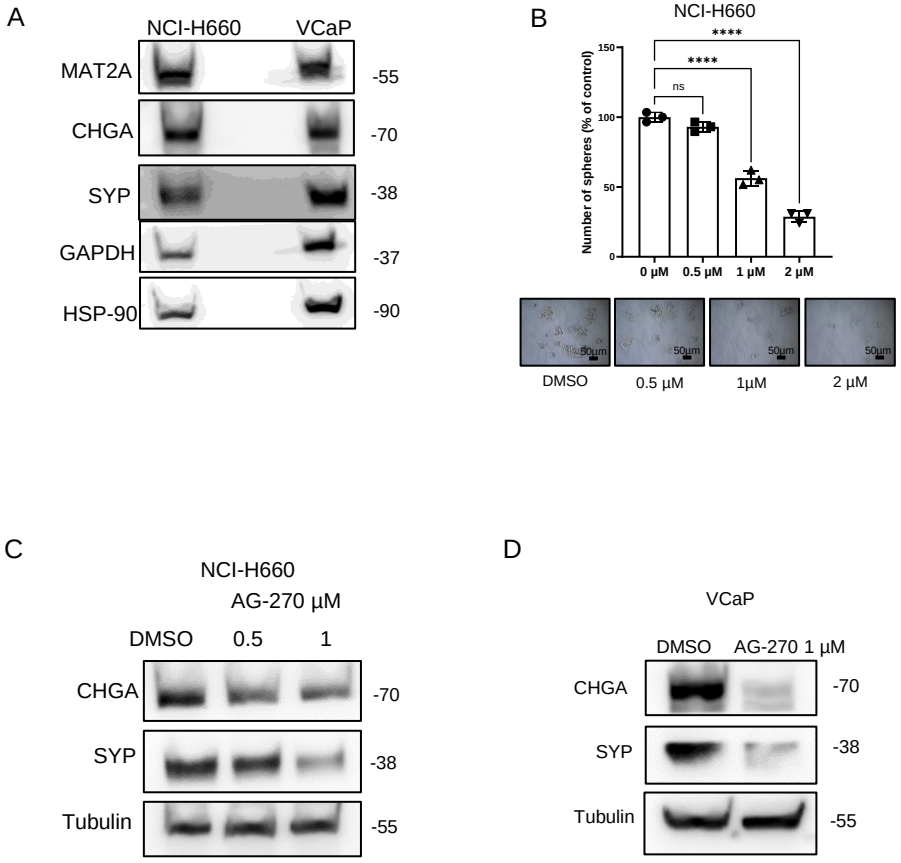

Supplementary Figure 9. NCI-H660 cells expresses MAT2A and are sensitive to MAT2Ai.
A) Immunoblot of selected markers in NCI-H660 and VCaP cells. B) Number of tumorspheres from NCI-H660 cells under treatment with the indicated concentration of AG-270 (n=3 biological replicates). Bottom, images of spheres. Scale bars are 50µm. C) Immunoblot of NE markers in NCI-H660 cells after indicated treatment. D) Immunoblot of selected NE markers in VCaP cells following treatment with AG-270. Molecular weights are indicated in kilodaltons (kDa). (Panels A, C and D, n=2 independent experiments). All error bars, mean ± s.d. n.s.=not significant, ****p < 0.0001. One-way-ANOVA was used to test significant differences between groups.

Supplementary Table 1.

	Plasmid	Ref. number	
	pCW57.1-MAT2A	100521	
	shRNA	Ref. number	Target sequence
	shMAT2A n.1	TRCN0000276466	CTGGCAGAACTACGCCGTAAT
	shMAT2A n.2	TRCN0000276407	GTTCAGGTCTCTTATGCTATT
	Construct for qRT-PCR	Target sequence	
	SOX2 forward	5' AGAACCCCAAGATGCACAAC 3'	
	SOX2 reverse	5' GCTTAGCCTCGTCGATGAAC 3'	
	NANOG forward	5' CAGAAGGCCTCAGCACCTAC 3'	
	NANOG reverse	5' ACTGGATGTTCTGGGTCTGG3'	
	AR forward	5’ CGGAAGCTGAAGAAACTTGG 3’	
	AR reverse	5’ ATGGGCTGACATTCATAGCC 3’	
	β-actin forward	5’ ATTGGCAATGAGCGGTTC 3’	
	β-actin reverse	5’ GGATGCCACAGGACTCCAT 3’	
	Construct for ChIP-PCR	Target sequence	
	NKX3.1 promoter forward	5’ TGCGGATAAAGGAACCACCA 3’	
	NKX3.1 promoter reverse	5’ AGGCATGACAAGTAGGTGCAGC 3’	
	CDK1 enhancer forward	5’ GGGAAAGAGAAGCCCTACACTTG 3’	
	CDK1 enhancer reverse	5’ GGGCTGTGCTACTTCTCTGGG 3’	
	UBE2C enhancer forward	5’ tgcctctgagtaggaacaggtaagt 3’	
	UBE2C enhancer reverse	5’ tgctttttccatcatggcag 3’	
	CDC20 enhancer forward	5’ ggagttgtgagaacacccgg 3’	
	CDC20 enhancer reverse	5’ aacacccaggtacaccctcg 3’	
	AR enhancer forward - set 1	5’ TGCCAGCACCAGTTTCTAGA 3’	
	AR enhancer reverse - set 1	5’ TAAGTGCCAAGCTTCCAGGT 3’	
	AR enhancer forward - set 2	5’ GAAAGGGAGTTGGGGCAAAT 3’	
	AR enhancer reverse - set 2	5’ CCCTGTTCTCAAAGTGCTGT 3’	